Calibration error analysis of electro-optical detection systems

Qijian Tang (汤其剑)[1,2,3], Xiangjun Wang (王向军)[1,3*], and Qingping Yang (杨清平)[2]

[1]*State Key Laboratory of Precision Measuring Technology and Instrument, Tianjin University, Tianjin 300072, China*

[2]*School of Engineering and Design, Brunel University, Uxbridge, Middlesex UB8 3PH, UK*

[3]*MOEMS Education Ministry Key Laboratory, Tianjin University, Tianjin 300072, China*

*Corresponding author: xdocuxjw@vip.163.com

We present detailed analysis of calibration process error for electro-optical detection systems, which can be simplified as the plane rotation around a non-orthogonal axis. By means of octonions it firstly proves that the plane rotation around a non-orthogonal axis can be decomposed into rotations around two perpendicular axes. The rotation is further divided into three steps, and the calibration error is hence discussed and obtained. The simulation and test results indicate that there are large calibration errors in calibration process. The pointing error can be effectively improved after separating error components, which provides a more accurate set data for further compensation.

OCIS codes: 120.0120, 120.3940.

doi: 10.3788/COL201412.121203.

Electro-optical detection systems (EODSs) are widely used to collect targets' location information in scientific, military, and commercial applications. They are often installed on vehicles, ships, aircrafts, and spacecraft[1–3]. The pointing accuracy as a critical parameter significantly affects the location accuracy because of the pointing error introduced by axial misalignments, non-perpendicularity, etc., and it is thus necessary to determine and compensate for the pointing error[4]. Laser tracker and autocollimator are a kind of automated precision optical instrument for the non-contact measurement of small angles[5,6], which can be used in the calibration process of EODS, especially the autocollimator[4,7]. As shown in Fig. 1, the plane mirror is fixed on the inner gimbal of EODS, which is fixed on a high precision turntable. When the EODS generates the azimuth angle θ_A and elevation angle θ_E, the turntable rotates the same angles in opposite directions, respectively. The autocollimator will present the angle biases in horizontal and vertical directions, Δ_A and Δ_E. If the elevation bias is zero ($\Delta\theta_E = 0$), and the azimuthal bias $\Delta\theta_A$ is minor, then

$$\Delta_A = \Delta\theta_A \cos\theta_E, \left(-\frac{\pi}{2} \le \theta_E \le \frac{\pi}{2}\right). \qquad (1)$$

If $\theta_E \ne 0$, $\Delta_A \ne \Delta\theta_A$. It is mainly because the mirror is no longer parallel to the azimuth axis. And the azimuth rotation problem with an elevation is equivalent to a plane rotation around a non-orthogonal axis. Further, in some applications, it is very difficult to guarantee calibration apparatus as shown in Fig. 1, leading to more serious calibration process error. Hence, it is necessary to determine the calibration process error. Note that geometric error compensation of EODS is not discussed here.

It is well known that quaternions can be used to speed up calculations involving rotations. A quaternion is represented by just four scalars, in contrast to a 3×3 rotation matrix which has nine scalar entries[8]. Since invented by Hamilton in 1843, quaternions have been widely used in situations involving rotations. Octonions, which were discovered independently by Cayley in 1845, are not widely used as quaternions. One of the most familiar applications is to describe the process whereby an electron emits or absorbs a photon[9], where it can be used to describe the spinor.

The octonions are an 8-dimensional algebra with basis **1**, ***i***, ***j***, ***k***, ***l***, ***il***, ***jl***, and ***kl***. Octonions are non-associative as $(ij)l = -i(jl) = kl \ne i(jl)$. An arbitrary octonion can be described as

$$O = a_0 + a_1\boldsymbol{i} + a_2\boldsymbol{j} + a_3\boldsymbol{k} + a_4\boldsymbol{l} + a_5\boldsymbol{il} + a_6\boldsymbol{jl} + a_7\boldsymbol{kl}, \qquad (2)$$
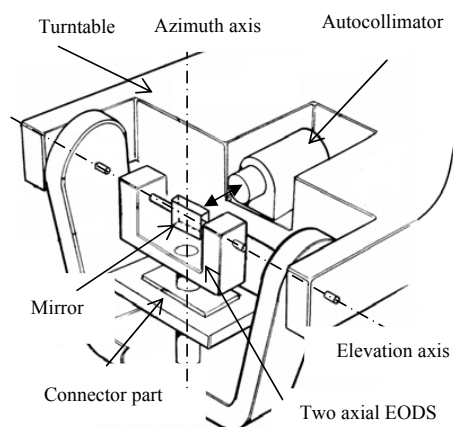

Fig. 1. Calibration system of EODS.

where $a_0 - a_7$ are real numbers.

Suppose $\boldsymbol{p}$ is a vector, it rotates 2θ around an axis $\boldsymbol{n}$ to $\boldsymbol{q}$, define $Q_n = \cos\theta + \boldsymbol{e}_n\sin\theta$, Q_n^* is the conjugate of Q_n. $\boldsymbol{e}_n$ is the unit vector of $\boldsymbol{n}$. And $\boldsymbol{q}$ can be calculated as

$$\boldsymbol{q} = Q_n \boldsymbol{p} Q_n^*. \tag{3}$$

Suppose O_8 is an octonion, Q_4 is a quaternion and its conjugate Q_4^*, it is facile to find

$$O = Q_4 O_8 Q_4^* = (Q_4 O_8)Q_4^* = Q_4(O_8 Q_4^*). \tag{4}$$

Similar to Eq. (3), the first four items of octonions in Eq. (2) are just a quaternion, of which the result can represent a spatial position rotation. Through relevant computations, the results in Eq. (4) can denote rotation process, including position rotating and spinning. In the following, computations with Eq. (4) only involve last four items of octonions. In an arbitrary coordinate system OXYZ, we assume the basis of OX are $\boldsymbol{i}$ and $\boldsymbol{il}$, that of OY are $\boldsymbol{j}$ and $\boldsymbol{jl}$, and that of OZ are $\boldsymbol{k}$ and $\boldsymbol{kl}$.

We have realized the decomposition of the rotation axis into two perpendicular axes in non-orthogonal rotation of a vector in other papers. In the actual calibration process of EODS, the factor affecting autocollimator readout accuracy is the mirror's rotation. It involves the plane rotation around a non-orthogonal axis. Take the plane Ω and line $\overline{OP}$ as the mirror and azimuth axis of EODS in Fig. 1, respectively. If the elevation angles of EODS and turntable are α and $-\alpha$, respectively, the mathematical model can be established as shown in Fig. 2.

Assume the plane Ω will rotate 2θ around $\overline{OP}$, which has an inclined angle α with Ω. $\overline{OC}$ is the projection of $\overline{OP}$ in Ω. And we establish the coordinate system OXYZ, $\overline{OA}$ is an arbitrary vector in Ω, which has an inclined angle β with $\overline{OC}$. We define the inclined angle between $\overline{OP}$ and $\overline{OA}$ as η and establish the coordinate system $OX_1Y_1Z_1$ which is based on the plane AOP. Assuming $O_{OA} = \boldsymbol{jl}$, we can obtain the rotated octonion.

$$O_1 = Q_{OP}O_{OA}Q_{OP}^* = -\sin 2\theta \cos\eta\boldsymbol{l} + \cos 2\theta\boldsymbol{jl} + \sin 2\theta \sin\eta\boldsymbol{il}, \tag{5}$$

where $Q_{OP} = \cos\theta + (\cos\eta\boldsymbol{j} + \sin\eta\boldsymbol{k})\sin\theta$.

In another coordinate system OX_2Y_1Z based on the plane AOZ, we will try to decompose the rotation around $\overline{OP}$ into spinning around $\overline{OC}$ and rotating around $\overline{OD}$. We define
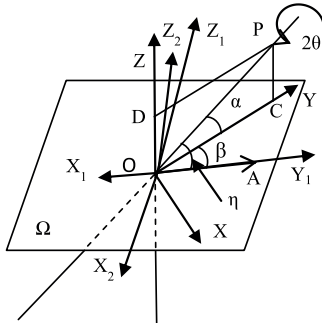
two respective angles as $2\delta'$ and $2\gamma'$. The corresponding quaternions are $Q_{OY} = \cos\delta' + \sin\delta'(-\sin\beta\boldsymbol{i} + \cos\beta\boldsymbol{j})$ and $Q_{OZ} = \cos\gamma' + \sin\gamma'\boldsymbol{k}$. Combining the two quaternions, we have

$$Q_{OYZ} = \cos\theta + \sin\delta'(-\sin\beta\boldsymbol{i} + \cos\beta\boldsymbol{j}) + \sin\gamma'\boldsymbol{k}, \tag{6}$$

where $\sin^2\theta = \sin^2\delta' + \sin^2\gamma'$. We can obtain the decomposed rotation octonion as

$$O_2 = Q_{OYZ}O_{OA}Q_{OYZ}^* = -2\sin\delta'\cos\beta\cos\theta\boldsymbol{l} + \cos 2\theta\boldsymbol{jl} + \left(2\sin\gamma'\cos\theta\boldsymbol{il} + 2\sin\delta'\sin\beta\cos\theta\boldsymbol{kl}\right). \tag{7}$$

From $O_1 = O_2$ and $\cos\eta = \cos a\cos\beta$, we finally obtain the angles

$$\begin{cases} 2\delta' = 2\sin^{-1}\left(\sin\theta\cos a\right), \\ 2\gamma' = 2\sin^{-1}\left(\sin\theta\sin a\right). \end{cases} \tag{8}$$

Equation (8) indicates that the rotation decomposition is independent of β, which means the plane rotation can be divided into rotations around two perpendicular axes. However, $2\delta'$ is not the real spinning angle, it can be shown that the real spinning angle is given by

$$2\delta_0 = 2\sin^{-1}\left(\frac{\sin\theta\cos a}{\sqrt{1 - \sin^2\theta\sin^2 a}}\right). \tag{9}$$

Meanwhile, the rotation of the angle $2\gamma'$ is around an axis $\overline{OZ_2}$ which has an inclined angle δ_0 with $\overline{OD}$, and $\overline{OD}$ is its projection in the plane YOZ. We can hence divide the rotation process into three steps: spinning δ_0, rotating $2\gamma'$, and spinning δ_0.

As presented in Fig. 3, the plane Ω_1 rotates 2θ around $\overline{OP}$ to Ω_2. Figure 3(left) shows the rotation impact on the autocollimator and Fig. 3(right) shows the mirror rotation decomposition. And $\overline{OPC_1}\perp\Omega_1$, $\overline{OPC_2}\perp\Omega_2$, $\overline{OD_1}\perp\Omega_1$, $\overline{OD_2}\perp C_1OC_2$, $\overline{OD_1}\perp\Omega_3$, $\overline{QC_1}\perp\overline{OQ}$, $\overline{QC_2}\perp\overline{OQ}$, $\overline{PC_1}\perp\overline{OC_1}$, $\overline{PC_2}\perp\overline{OC_2}$, $\angle C_1QC_2 = 2\theta$, $\angle POC_1 = \angle POC_2 = a$. The inclined angle between Ω_1
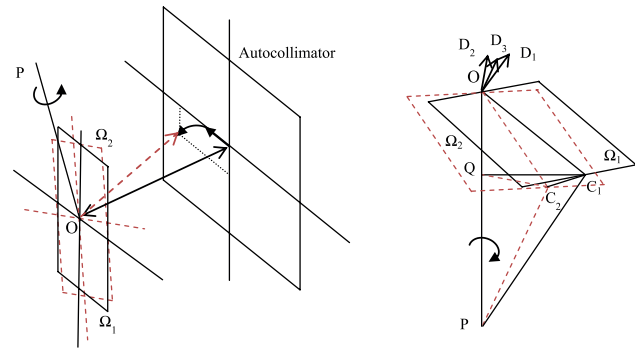

Fig. 2. Arbitrary non-orthogonal plane rotation.

Fig. 3. Plane rotation diagram.

and C_1OC_2 is δ_0, hence, the plane rotation around $\overline{OP}$ in Fig. 3 can be divided as follows:

(1) Ω_1 spins δ_0 around $\overline{OC_1}$ to C_1OC_2, $\angle D_1OD_2 = \delta_0$.

(2) C_1OC_2 rotates $2\gamma'$ around $\overline{OD_2}$, $\angle C_1OC_2 = 2\gamma'$.

(3) C_1OC_2 spins δ_0 around $\overline{OC_2}$ to Ω_2, $\angle D_2OD_3 = \delta_0$.

As the autocollimator readout is dependent on the rotation of reflecting mirror, in the first step of rotation decomposition, the autocollimator readout will change in the horizontal direction, and the value is

$$\theta_1 = \delta_0 = \sin^{-1}\left(\frac{\sin\theta\cos a}{\sqrt{1-\sin^2\theta\sin^2 a}}\right). \tag{10}$$

In the second step, the mirror spins, the readout remains the same. In the third step, the mirror rotates δ_0 around a slant axis, of which the inclined angle with the vertical axis is $2\gamma'$. The equivalent rotation angle in the horizontal direction is given by

$$\theta_2 = \frac{1}{2}\tan^{-1}(\tan 2\delta_0 \cos 2\gamma'). \tag{11}$$

As to the azimuth calibration, the non-orthogonal rotation of 2θ around $\overline{OP}$ is equivalent to the rotation of $(\theta_1+\theta_2)$ around the vertical axis, and the rotation error θ_e is

$$\theta_e = 2\theta - (\theta_1+\theta_2) \tag{12}$$

Assume the rotated angle 2θ is $-40°-40°$ and the inclined angle α is $-30°-30°$, according to Eq. (12), the rotation error is shown in Fig. 4, which indicates that the rotation error becomes serious as θ and α increase.

Hence, the rotation bias of azimuth in Fig. 1 and Eq. (1) can be rewritten as

$$\Delta_A = \theta_1 + \theta_2 = f(\Delta\theta_A, \theta_E) = \sin^{-1}\left(\frac{\sin\frac{\Delta\theta_A}{2}\cos\theta_E}{\sqrt{1-\sin^2\frac{\Delta\theta_A}{2}\sin^2\theta_E}}\right)$$

$$+\frac{1}{2}\tan^{-1}\left\{\tan\left[2\sin^{-1}\left(\frac{\sin\frac{\Delta\theta_A}{2}\cos\theta_E}{\sqrt{1-\sin^2\frac{\Delta\theta_A}{2}\sin^2\theta_E}}\right)\right]\right.$$

$$\left.\cos\left[2\sin^{-1}\left(\sin\frac{\Delta\theta_A}{2}\sin\theta_E\right)\right]\right\}. \tag{13}$$

The actual calibration apparatus is shown in Fig. 5. The angular range is $-20°-20°$ for azimuth, and $-20°-10°$ for elevation. The calibration process can be described as follows: the EODS rotates θ_E around its elevation axis, the turntable rotates $-\theta_E$ around its elevation axis, then the EODS rotates θ_{A1} around its azimuth axis, the turntable rotates $-\theta_{A2}$ around its azimuth axis. The autocollimator readout of azimuth is $\Delta_{A'}$, assuming the elevation bias is zero, from Eqs. (11) to (13), we can obtain

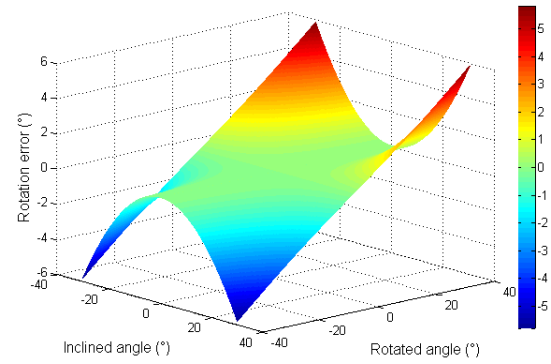$$\Delta_{A'} = -\theta_{A2} + f\left(\theta_{A1}, \theta_E\right). \tag{14}$$
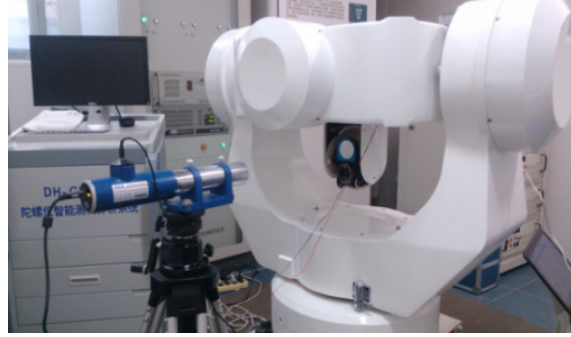

Fig. 4. Rotation error.

Fig. 5. EODS calibration apparatus.

Figure 6 presents the test results before and after removing the calibration process error, with the error variance decreasing from $0.138(°)^2$ to $0.048(°)^2$. Figures 4 and 6 demonstrate that the calibration methods presented in Figs. 1 and 5 can introduce serious error in the calibration process.

In conclusion, we establish a mathematical model for the calibration of EODS. The nature of the problem is attributed to plane rotation around a non-orthogonal axis. It is proved that plane rotation can be decomposed into rotations around two perpendicular axes by means of octonions. We then realize the decomposition in three steps and finally obtain the calibration process error presented in Eqs. (13) and (14). The test results demonstrate that the calibration method can introduce significant error in pointing accuracy. With the error component equations,
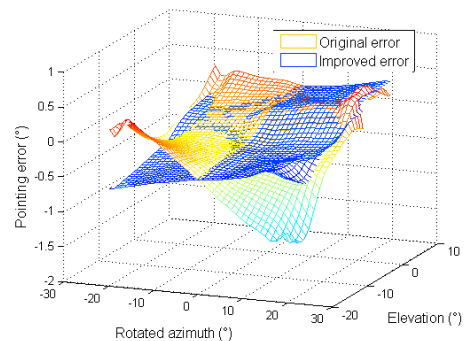

Fig. 6. Pointing error of azimuth.

the error is effectively separated, which guarantees the test data accuracy for further compensation.

References

1. J. Hilkert, IEEE Control Syst. Mag. **28,** 26 (2008).
2. K. Michael, IEEE Control Syst. Mag. **28,** 47 (2008).
3. Q. Yang, X. Zeng, and B. Zhao, Chin. Opt. Lett. **11,** 061202 (2013).
4. A. Rue, IEEE Trans. Aerosp. Electron. Syst. **AES-6,** 697 (1970).
5. M. Gao, Z. Dong, Z. Bian, Q. Ye, Z. Fang, and R. Qu, Chin. Opt. Lett. **9,** 091201 (2011).
6. J. Li and S. Wu, Chin. Opt. Lett. **11,** 091202 (2013).
7. Z. Zhang, X. Zhou, and D. Fan, Acta Aeronaut. Astronaut. Sin. **32,** 2042 (2011).
8. R. Goldman, Graph. Models **73,** 21 (2011).
9. J. Baez, Bull. Am. Math. Soc. **39,** 145 (2001).